Journal of Science Research and Reviews
PRINT ISSN: 1595-9074
E-ISSN: 1595-8329
DOI: https://doi.org/10.70882/josrar.2026.v3i3.216
Homepage: https://josrar.esrgngr.org
Original Research Article

Numerical Investigation of a Fractional-Order Dengue Fever Model via the Generalized Adams–Bashforth–Moulton Technique

[1,2]Enejoh Jalija, *[1]Jeremiah Amos, [1]David Omale, [1]William Atokolo, [2]Benjamin Adamu, [3]Eunice Ajifa Isah, [1]Emmanuel Abah and [1]Bolarinwa Bolaji

[1]Department of Mathematical Sciences, Prince Abubakar Audu University, Anyigba, Nigeria
[2]Department of Mathematics and statistics, The Federal Polytechnic Idah, Nigeria
[3]Department of Economics, Prince Abubakar Audu University, Anyigba, Nigeria
*Corresponding Author's email: amosjeremiah1997@gmail.com

KEYWORDS
Dengue fever,
Fractional,
Adam-Bashforth-Moulton,
Transmission,
Control,
Strategies.

ABSTRACT
The rapid transmission and the increasing prevalence of Dengue fever make it a great public health challenge in the world, especially in tropical and subtropical regions. For this study, a fractional-order mathematical model was formulated to study the Dengue fever transmission dynamics and control. Important epidemiological parameters, including vaccination, treatment, and effective contact rates, were included in the model. Qualitative analysis confirmed that the model solutions exist, are unique, positive, and bounded, and that the basic reproduction number is computable to determine the conditions for the persistence and control of the disease. They found that higher vaccination and treatment coverage translates into decreased transmission and the reproduction number becoming less than 1, which is a good indicator of disease elimination. On the other hand, high contact rates were seen to be favorable for the spread and persistence of the infection. The analytical results were also supported with numerical simulations, contour plots, and surface plots, which showed that the prevalence of Dengue fever can only be reduced if intervention strategies are implemented in all aspects, such as vaccination, treatment, vector control, and reduction of transmission pathways. The results of this study help to understand the dynamics of Dengue transmission and offer valuable information to policy makers, health workers, and researchers for prevention, control, and potentially eradication of Dengue fever in endemic areas in the context of achieving sustainable solutions.

CITATION
Jalija, E., Amos, J., Omale, D., Atokolo, W., Adamu, B., Isah, E. A., Abah, E., & Bolaji, B. (2026). Numerical Investigation of a Fractional-Order Dengue Fever Model via the Generalized Adams–Bashforth–Moulton Technique. *Journal of Science Research and Reviews*, *3*(3), 164-178. https://doi.org/10.70882/josrar.2026.v3i3.216.

INTRODUCTION

Dengue fever is a vector-borne virus disease and is caused by a virus called the dengue virus. The virus is classified in the Flavivirus family and is comprised of four serotypes (DENV-1, DENV-2, DENV-3 and DENV-4) (Gubler, 1998). Dengue fever is a significant public health problem and is widely spread throughout tropical and subtropical areas of the worldwide. The disease is endemic in Western Pacific regions (particularly), Southeast Asia, Eastern Mediterranean and Americas (World Health Organization [WHO], 2018; Bhatt et al. 2013). According to Bhatt et al. (2013), more than 390 million people are infected with Dengue virus annually and Dengue fever is one of the fastest spreading mosquito-borne viral diseases in the

world. Now, more than 100 countries around the world are affected by Dengue fever (Brady et al., 2012).

Dengue fever is spread to humans via infected female Aedes mosquitoes, particularly Aedes aegypti (Dengue Virus Net, 2019). In some people infected, the disease can manifest as a mild infection or as Dengue haemorrhagic fever (DHF) and Dengue shock syndrome (DSS), which may cause death without proper treatment (Halstead et al., 1970). According to the World Health Organization (2019), over the years there has been a dramatic rise in the number of cases of severe Dengue, especially Dengue hemorrhagic fever, which is having a great impact on health systems around the world.

Dengue virus is transmitted by an infected mosquito with the virus attached when a susceptible person gets bitten by it (Dengue virus Net, 2019). After recovery from an infection with one serotype of Dengue virus, there is partial or complete immunity to that serotype, but infection with other serotypes can still occur (Halstead et al., 1970). Although various attempts have been made to find antiviral specific treatment for Dengue fever, there is none other than supportive care (such as fluid replacement therapy) and symptomatic treatment (Dengue virus Net, 2018). Moreover, despite significant advances in Dengue vaccine research, a completely effective and widespread vaccine is still a challenge (World Health Organization, 2017). The World Health Organization (2017) reported that efforts around the world to develop a vaccine for Dengue have been stepped up over the last few years, and that Mexico was one of the first countries to approve a Dengue vaccine for use in the public population.

The focus of researchers now is on fractional calculus since fractional derivatives support expert knowledge of the dynamics of physical systems as indicated by Atokolo et al. (2022). In the fractional order system model, total systems are described and not local systems as used by the integer order system models. This type of modelling provides a more accurate description of systems with memory Atokolo et al (2022).

Fractional order models are preferred in terms of realistic and practicality compared to integer order models. Singular kernel fractional derivatives such as the Riemann-Liouville derivative and Caputo derivative are used in biological problems. The Atangana-Baleanu operator as well as Mittag-Leffler operator is part of the non-singular type of derivative. Atokolo et al (2022), used the technique of LADM to control Zika virus infection using a fractional order sterile insect technology (SIT) whose solutions were given in the form of converging infinite series, giving exact solutions. Atokolo et al (2024) showed a fractional order mathematical model of the epidemiological parameters of the Lassa fever viral infection, and used a fractional order derivative with a power law function to investigate the impact of treatment and vaccination on the dynamics of the viral spread of Lassa fever. Yunus et al (2023), investigated the COVID-19 spread in Nigeria using LADM and Caputo fractional-order derivative, which confirmed that recovery rates in normal situations were higher due to the provision of treatment and vaccinations. Omede et al (2024) formulated a fractional order model for Soil Transmitted Helminth (STH) infection incorporating the Caputo derivative and solved it by the use of LADM series solution. Their study confirmed that the series convergence results in the accuracy solution and the fractional order model is more flexible than the standard model. Amos et al (2024) developed a fractional mathematical model of hepatitis C transmission dynamics through contact rates and treatment and also created the Adams-Bash-forth Moulton method which showed that the disease can be reduced by decreasing the contact rates, increasing the treatment rates and the fractional model is more flexible than the standard model. Ahmed et al (2021), created a prediction model for the co-epidemic of HIV and COVID-19 transmissions based on ABC-fractional order derivative.

The study by Omame et al (2022), studied a fractional order model of co-infection of hepatitis B virus and COVID-19 with Atangana-Baleanu derivative and concluded that prevention is the only way to control the disease. Acheneje et al (2024), developed a fractional order transmission dynamics model for the co- infection of COVID-19 and Monkey pox and used LADM for an approximate solution and real data fitting as well. The investigation showed that the development of additional treatment facilities would decrease the disease cases. Smith et al (2023), studied Modeling on the Co- infection Dynamics of Hepatitis C and COVID-19 by reviewing recent mathematical modeling studies of hepatitis C and COVID-19 co-infection. The review discusses the standard modelling procedure and important results of interest, and suggests new areas for research. Atokolo et al. (2023), created a mathematical model for the transmission of vector-borne diseases with vertical transmission and prevention.

Their advantages are mainly attributed to the simultaneous flexibility and non-locality aspects of fractional order models. Data can be better modelled by using fractional derivatives because of their flexibility, compared to classical derivatives. These derivatives can offer advantages by their ability to measure non-locality that classical derivatives can't. By means of their fractional operator, fractional order models have a memory property that classical models do not exhibit. Nowadays, Fractional differential equations are employed as a method in the solution of problems by the modern scientists. Ullah et al (2020), presented research which Das et al (2024), described about the solution of fuzzy Volterra integral equations with degenerate kernels, by employing a combination method. Researchers have combined the Laplace transform method with Adomian Decomposition

for advancing the theory of fuzzy analytical dynamic equations due to their great impact in this area.

The study is of keen interest because of the discovery of insights for fuzzy analytical dynamic equation theory. Ali et al (2017) studied three point boundary value problem with respect to its existence and stability analysis. Using a non-linear fractional approach, the authors analysed several types of Ulam stability.

There are various mathematic models used for control and analysis of infectious diseases, in particular, Dengue fever. The Laplace-Adomain Transformation Method has been employed to obtain approximate solutions for Lassa fever models of fractional orders and the fractional-order model has been developed to investigate the dynamics of the spread of HIV/AIDS and COVID-19. Fractional-order models are used to study the impacts of antiretroviral therapy (ART) using novel type-2 fuzzy logic controllers in Dengue fever models.

The fractional-order models are very useful because of their superior flexibility, non-locality and memory effects. Fractional derivatives result in better models in data fitting as they are more flexible and accurate than classical derivatives. Models show proficiency in exhibiting memory effects which classical models cannot. In recent studies, researchers Ullah et al (2020), and Ali et al (2017) have shown that there is a growing interest in applications of fractional calculus for modeling of complex systems due to their research on fuzzy Volterra integral equations and stability in three-point boundary value problems.

In this paper, we first give sufficient conditions for existence and uniqueness of the solutions of a fractional-order Dengue fever model, do stability analysis of the endemic equilibrium by using the Lyapunov function method, numerically solve the model by using the fractional Adams–Bashforth–Moulton method and simulate the model to show the dynamics of the model.

A thorough review of existing literature reveals that the literature has not incorporated the fractional calculus with Adams-Bashforth-Moulton method for the study of the Dengue fever disease and its control.

Definition 1: Let $f \in \Lambda^{\infty}(R)$,The left and right Caputo fractional derivatives of the function$f$ are then defined as:

$${}^{c}D_t^{\vartheta} f(t) = \left(t^{0}D_t^{-(-n\vartheta)}\left(\frac{d}{dt}\right)^{n} f(t)\right)$$

$${}^{c}D_t^{\vartheta} f(t) = \frac{1}{\Gamma(n-\vartheta)}\int_0^t \left((t-\lambda)^{n-\vartheta-1} f^{n}(\lambda)\right) d\lambda \qquad (1)$$

Similarly

$${}_{T}^{c}D_t^{\vartheta} f(t) = \left({}_{t}D_T^{-(n-\vartheta)}\left(\frac{-d}{dt}\right)^{n} f(t)\right)$$

$${}_{T}^{c}D_t^{\vartheta} f(t) = \frac{(-1)^{n}}{\Gamma(n-\vartheta)}\int_t^T \left((\lambda-t)^{n-\vartheta-1} f^{n}(\lambda)\right) d\lambda,$$

Definition 2: The generalized Mittag-Leffler function $E_{\vartheta,\beta}(x)$ for $x \in R$ is given by:

$$E_{\vartheta,\beta}(x) = \sum_{n=0}^{\infty} \frac{x^{n}}{\Gamma(\vartheta n+\beta)}, \vartheta, \beta > 0, \qquad (2)$$

which can be denoted as;

$$E_{\vartheta,\beta}(x) = xE_{\vartheta,\vartheta\frac{x-\mu}{\vartheta}+\beta(x)} + \frac{1}{\Gamma(\beta)}, \qquad (3)$$

$$E_{\vartheta,\beta}(x) = L\left[t^{\beta-1}E_{\vartheta},\beta\left(\pm\omega t^{\vartheta}\right)\right] = \frac{S^{\vartheta-\beta}}{S^{\vartheta}\pm\omega}, \qquad (3.1)$$

Proposition 1

Let $f \in \Lambda^{\infty}(R) \cap C(R)$ and $\vartheta \in R, n-1 < \vartheta < n$,

Therefore, the conditions given below is satisfied:

1. ${}_{t_0}^{c}D_t^{\vartheta} I^{\vartheta} f(t) = f(t),,$ (3.2)

2. $I_{t_0}^{\vartheta} D_t^{\vartheta} f(t) = f(t) - \sum_{k=0}^{n-k} \frac{t^{k}}{k!} f^{k}(t_o).$ (4)

Model Formulation

The integer-order model classifies the Dengue fever infected individuals into eight categories: Susceptible humans (S_H), Exposed individuals (E_H), Dengue fever infected individuals (I_H), individuals receiving Dengue fever treatment $(T_H),,$ Vaccinated human population against Dengue fever (V_H) , Recovered human population from Dengue fever (R_H), susceptible vectors (S_V) , and infected vectors (I_V).

Susceptible humans to Dengue fever (S_H) are recruited at the rate of (Λ_H), The group decreases due to the natural death rate among humans $(\mu_H)$and vaccination at the rate of (σ_2), the recovery rate due to treatment is denoted as (ω) , the rate at which recovered individuals become susceptible again is represented as ρ , and vaccine failure rate (σ_1) , Several parameters influencing the susceptible humans are (β_H, β_V) respectively.

Therefore, we write the dynamics of susceptible individuals as follows:

$$\frac{dS_H}{dt} = \Lambda_H + \rho R_H + \sigma_1 V_H - \lambda_H S_H - (\sigma_2 + \mu_H) S_H,$$

Dengue fever exposed humans (E_H): the population is seeing more new cases and the infection rate $(\beta_H, \beta_V)$is increasing by respectively. The rate of decline of this class is given by the rate at which exposed humans become fully infected with Dengue fever(α), and the natural death rate(μ_H).

The dynamics of this population is presented here as:

$$\frac{dE_H}{dt} = \lambda_H S_H - (\alpha + \mu_H) E_H,$$

Dengue fever Infected humans (I_H): The number keeps increasing because Dengue fever sufferers pass the disease on to others at the rate of (α) , Natural death rate (μ_H)causes the human population size to decrease , Tropical diseases like dengue fever, led to human deaths at given death rates(δ) , and treatment rate (θ) of infected humans .

The dynamics of this population is described here by:

$$\frac{dI_H}{dt} = \alpha E_H - (\theta + \delta + \mu_H) I_H,$$

The growth of human infected with Dengue fever receiving treatment (T_H)depends on number of human infected with Dengue fever receiving treatment at rate (θ),The populations sizes decrease as people are cured of their Dengue fever infections by treatment at the rate of (ω) .The modification parameter that accounts for the decrease in

the rate at which humans on treatment die due to the Dengue fever is denoted by ϕ. The death rate of humans on treatment and natural death rate induced by the diseases are (δ) and μ_H respectively.

The dynamics of this population is then given by:

$\frac{dT_H}{dt} = \theta I_H - (\omega + \phi\delta + \mu_H)T_H,$

Vaccinated human population against Dengue fever(V_H)**:** When vaccination rates (σ_2) drop, the number of people who can still be infected with Dengue goes up. Over time, this vaccinated population shrinks due to natural death rate $(\mu_H)$and the gradual loss of vaccine protection (waning immunity) at the rate of(σ_1).

The way this population changes over time is described below:

$\frac{dV_H}{dt} = \sigma_2 S_H - (\sigma_1 + \mu_H)V_H,$

Recovered human population from Dengue fever(R_H): The number of recovered individuals depends largely on the recovery rate (ω) of those receiving treatment. However, this population declines due to natural death rate of (μ_H) and the rate at which recovered people lose immunity and become susceptible again which affects how soon they might relapse back into an infection at the rate of (ρ).

Here's how this population changes over time:

$\frac{dR_H}{dt} = \omega T_H - (\rho + \mu_H)R_H,$

Susceptible vector population(S_V)**:** New susceptible vectors are added at a recruitment rate (Λ_V). This group shrinks due to two main factors: the rate at which vectors bite humansβ_V, and the natural death rate among the vector population (μ_V).

The dynamics of this population are described as follows:

$\frac{dS_V}{dt} = \Lambda_V - \lambda_V S_V - \mu_V S_V,$

Infected vector population(I_V)**:** This group grows as vectors bite humans at a certain rate (β_V). However, it also shrinks due to two factors: death caused by the attempt to bite infected humans(δ_V), and the natural death rate (μ_V)among the vector population.

The dynamics of this population are presented as follows:

$\frac{dI_V}{dt} = \lambda_V S_V - (\delta_V + \mu_h)I_V.$

Dengue fever Model Flow Diagram

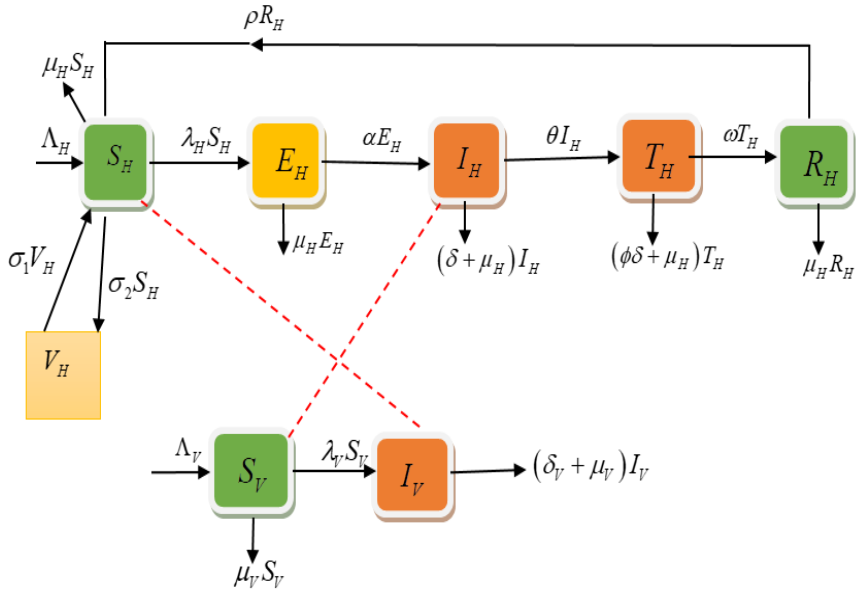

Figure1: Dengue fever model flow Diagram

The Dengue fever transmission dynamics model is shown in the flow diagram (Figure 1). It shows how people move between various epidemiological compartments from susceptible (exposed with effective contact with infected people) to infected to symptomatic to hospitalize to recover to deceased. The exposed persons go on to be infectious. Treatment, vaccinations and transitions related to the recovery or death of individuals are also included, along with the population of susceptible vectors and the population of infected vectors, which represents disease progression and intervention measures. The diagram clearly depicts the role of infection, progression, treatment, vaccination and natural removal rates in the transmission of Dengue fever.

Model Equation

$$\begin{aligned}
\frac{dS_H}{dt} &= \Lambda_H + \rho R_H + \sigma_1 V_H - \lambda_H S_H - (\sigma_2 + \mu_H)S_H,\\
\frac{dE_H}{dt} &= \lambda_H S_H - (\alpha + \mu_H)E_H\\
\frac{dI_H}{dt} &= \alpha E_H - (\theta + \delta + \mu_H)I_H,\\
\frac{dT_H}{dt} &= \theta I_H - (\omega + \phi\delta + \mu_H)T_H,\\
\frac{dV_H}{dt} &= \sigma_2 S_H - (\sigma_1 + \mu_H)V_H,\\
\frac{dR_H}{dt} &= \omega T_H - (\rho + \mu_H)R_H,
\end{aligned} \qquad (5)$$

$\frac{dS_V}{dt} = \Lambda_h - \lambda_V S_V - \mu_V S_V,$
$\frac{dI_V}{dt} = \lambda_V S_V - (\delta_V + \mu_V) I_V.$
Where$\lambda_H = \frac{b\beta_H I_V}{N_H}$and $\lambda_V = \frac{\beta_V I_H}{N_H}$.

Fractional order mathematical model

In this section, we transform integer-order model to fractional-order as seen below:

$$^{C}D_t^{\vartheta} S_H = \Lambda_H + \rho R_H + \sigma_1 V_H - \frac{b\beta_H I_V}{N_H} S_H - (\sigma_2 + \mu_H) S_H,$$

$$\begin{aligned}
^{C}D_t^{\vartheta} E_H &= \frac{b\beta_H I_V}{N_H} S_H - (\alpha + \mu_H) E_H,\\
^{C}D_t^{\vartheta} I_H &= \alpha E_H - (\theta + \delta + \mu_H) I_H,\\
^{C}D_t^{\vartheta} T_H &= \theta I_H - (\omega + \phi\delta + \mu_H) T_H,\\
^{C}D_t^{\vartheta} V_H &= \sigma_2 S_H - (\sigma_1 + \mu_H) V_H,\\
^{C}D_t^{\vartheta} R_H &= \omega T_H - (\rho + \mu_H) R_H,\\
^{C}D_t^{\vartheta} S_V &= \Lambda_V - \frac{\beta_V I_H}{N_H} S_V - \mu_V S_V,\\
^{C}D_t^{\vartheta} I_V &= \frac{\beta_V I_H}{N_H} S_V - (\delta_V + \mu_V) I_V.
\end{aligned} \quad (6)$$

Subject to the initial conditions
$S_H(0) = S_{H0}, E_H(0) = E_{H0}, I_H(0) = I_{H0}, T_H(0) = T_{H0}, V_H(0) = V_{H0}, R_H(0) = R_{H0}, S_V(0) = S_{V0}, I_V(0) = I_{V0}.$

Model Analysis

Positivity of model solution

We considered the human population non-negativity of the initial values,
$N_H(t) \le \frac{\Lambda_H}{\mu_H}$ as $t \to \infty$
Secondly, $if\ limsup\, N_{H0}(t) \le \frac{\Lambda_H}{\mu_H}$, then our model feasible domain is given by:
$\Omega_H = \left\{(S_H, E_H, I_H, T_H, V_H, R_H) \subset R_+^6 : S_H + E_H + I_H + T_H + V_H + R_H \le \frac{\Lambda_H}{\mu_H}, \right\}$, (7)
so that,
$\Omega = \Omega_H \subset R_+^6,$
Hence, Ω is positively invariant.
We also considered the vector population non-negativity of the initial values,
$N_V(t) \le \frac{\Lambda_V}{\mu_V}$ as $t \to \infty$
Secondly, $if\ limsup\, N_{V0}(t) \le \frac{\Lambda_V}{\mu_V}$, then our model feasible domain is given by:
$\Omega_V = \left\{(S_V, I_V) \subset R_+^2 : S_V + I_V \le \frac{\Lambda_V}{\mu_V}, \right\}$,
so that,
$\Omega = \Omega_V \subset R_+^2,$
Hence,Ω is positively invariant.
If $S_{H0}, E_{H0}, I_{H0}, T_{H0}, V_{H0}, R_{H0}$.are non-negative, then the solution of model (6) will be non-negative for t> 0. From Eq. (6), selecting the first equation, we obtained;

$$^{C}D_t^{\vartheta} S_H = \Lambda_H + \rho R_H + \sigma_1 V_H - \frac{b\beta_H I_V}{N_H} S_H - (\sigma_2 + \mu_H) S_H,$$

$$^{C}D_t^{\vartheta} S_H + \left(\frac{b\beta_H I_V}{N_H} + \sigma_2 + \mu_H\right) S_H = \Lambda_H + \rho R_H + \sigma_1 V_H,$$

But$\Lambda_H + \rho R_H + \sigma_1 V_H \ge 0$then,
$^{C}D_t^{\vartheta} S_H + \left(\frac{b\beta_H I_V}{N_H} + \sigma_2 + \mu_H\right) S_H \ge 0,$
Applying the Laplace transform we obtained:
$L\left[{}^{C}D_t^{\vartheta} S_H\right] + L\left[\left(\frac{b\beta_H I_V}{N_H} + \sigma_2 + \mu_H\right) S_H\right] \ge 0,$
$S_H^{\vartheta} S_H(s) - S_H^{\vartheta-1} S_H(0) + \left(\frac{b\beta_H I_V}{N_H} + \sigma_2 + \mu_H\right) S_H(s) \ge 0,$

$$S_H(s) \ge \frac{S_H^{\vartheta-1}}{S_H^{\vartheta} + \left(\frac{b\beta_H I_V}{N_H} + \sigma_2 + \mu_H\right)} S_H(0). \quad (8)$$

By taking the inverse Laplace transform, we obtained:
$$S_H(t) \ge E_{t\vartheta,1}\left(-\left(\frac{b\beta_H I_V}{N_H} + \sigma_2 + \mu_H\right) t^{\vartheta}\right) S_{H0}. \quad (9)$$

Now since the term on the right-hand side of Eq. (9) is positive, we conclude that $S_H \ge 0$ for$t \ge 0$. In the same way, we also have that $E_H \ge 0, I_H \ge 0, T_H \ge 0, V_H \ge 0, R_H \ge 0, S_V \ge 0, I_V \ge 0$. that is positives; therefore, the solution will remain in R_+^8 for all $t \ge 0$ with positive initial conditions.

Boundedness of fractional model solution

The total human population from our model is given by:
$N_H(t) = S_H(t) + E_H(t) + I_H(t) + T_H(t) + V_H(t) + R_H(t).$
So from our fractional model (6), we now obtain:
$cD_t^{\vartheta} N_H(t) = {}^{c}D_t^{\vartheta} S_H(t) + {}^{c}D_t^{\vartheta} E_H(t) + {}^{c}D_t^{\vartheta} I_H(t) + {}^{c}D_t^{\vartheta} T_H(t) + {}^{c}D_t^{\vartheta} V_H(t) + {}^{c}D_t^{\vartheta} R_H(t).$
$cD_t^{\vartheta} N_H(t) = \Lambda_H - \mu_H N_H(t)$ (10)
Taking the Laplace transformation of (10) we obtained;
$L\left[cD_t^{\vartheta} N_H(t)\right] = L[\Lambda_H - \mu_H N_H(t)],$
$S_H^{\vartheta} N_H(s) - S_H^{\vartheta-1} N_H(0) + \mu_H N_H(s) \le \frac{\Lambda_H}{\mu_H},$
$$N_H(s) \le \frac{S_H^{\vartheta-1}}{\left(S_H^{\vartheta} + \mu_H\right)} N_H(0) + \frac{\Lambda_H}{s_H\left(S_H^{\vartheta} + \mu_H\right)}, \quad (11)$$

By taking the inverse Laplace transform of Eq. (11) we obtained;
$N_H(t) \le E_{t\vartheta,1}\left(-\mu_H t^{\vartheta}\right) N_H(0) + \Lambda_H E_{t\vartheta,\vartheta+1}\left(-\mu_H t^{\vartheta}\right),$ (12)
At $t \to \infty$, the limit of Eq. (12) becomes
$\lim_{t\to\infty} Sup N_H(t) = \frac{\Lambda_H}{\mu_H}.$
This means that, if $N_{H0} \le \frac{\Lambda_H}{\mu_H}.$
then $N_H(t) \le \frac{\Lambda_H}{\mu_H}$which implies that,$N_H(t)$ is bounded.
We now conclude that, this region$\Omega = \Omega_H$, is well posed and equally feasible epidemiologically.

Existence and uniqueness of our model solution

Let the real non-negative be V we consider $U = [0, V[]]$

The set of all continuous function that is defined on P is represented by $N_e^0(V)$ with norm as;

$\|D\| = Sup\{|D(t)|, t \in V\}$.

Considering model (6) along with the initial conditions specified in (8), this can be represented as an initial value problem (IVP) in (13).

$$^{c}D_t^{\vartheta} D(t) = Z(t, D(t)), 0 < t < V < \infty, \quad (13)$$

$D(0) = D_0$.

Where $D(t) = \big(S_H(t), E_H(t), I_H(t), T_H(t), V_H(t), R_H(t), S_V(t), I_V(t)\big)$represents the classes and Z be a continuous function defined as follows:

$$Z(t, D(t)) = \begin{pmatrix} Z_1(t, S_H(t)) \\ Z_2(t, E_H(t)) \\ Z_3(t, I_H(t)) \\ Z_4(t, T_H(t)) \\ Z_5(t, V_H(t)) \\ Z_6(t, R_H(t)) \\ Z_7(t, S_V(t)) \\ Z_8(t, I_V(t)) \end{pmatrix} = \begin{pmatrix} \Lambda_H + \rho R_H + \sigma_1 V_H - \frac{b\beta_H I_V}{N_H} S_H - (\sigma_2 + \mu_H) S_H \\ \frac{b\beta_H I_V}{N_H} S_H - (\alpha + \mu_H) E_H \\ \alpha E_H - (\theta + \delta + \mu_H) I_H \\ \theta I_H - (\omega + \phi\delta + \mu_H) T_H \\ \sigma_2 S_H - (\sigma_1 + \mu_H) V_H \\ \omega T_H - (\rho + \mu_H) R_H \\ \Lambda_V - \frac{\beta_V I_H}{N_H} S_V - \mu_V S_V \\ \frac{\beta_V I_H}{N_H} S_V - (\delta_V + \mu_V) I_V \end{pmatrix}, \quad (14)$$

Using Proposition 1, we obtain:

$$\begin{aligned} S_H(t) &= S_{H0} + I_t^{\vartheta}\left[\Lambda_H + \rho R_H + \sigma_1 V_H - \frac{b\beta_H I_V}{N_H} S_H - (\sigma_2 + \mu_H) S_H\right], \\ E_H(t) &= E_{H0} + I_t^{\vartheta}\left[\frac{b\beta_H I_V}{N_H} S_H - (\alpha + \mu_H) E_H\right], \quad (15) \\ I_H(t) &= I_{H0} + I_t^{\vartheta}[\alpha E_H - (\theta + \delta + \mu_H) I_H], \\ T_H(t) &= T_{H0} + I_t^{\vartheta}[\theta I_H - (\omega + \phi\delta + \mu_H) T_H], \\ V_H(t) &= V_{H0} + I_t^{\vartheta}[\sigma_2 S_H - (\sigma_1 + \mu_H) V_H], \\ R_H(t) &= R_{H0} + I_t^{\vartheta}[\omega T_H - (\rho + \mu_H) R_H], \\ S_V(t) &= S_{V0} + I_t^{\vartheta}\left[\Lambda_V - \frac{\beta_V I_H}{N_H} S_V - \mu_V S_V\right], \\ I_V(t) &= I_{V0} + I_t^{\vartheta}\left[\frac{\beta_V I_H}{N_H} S_V - (\delta_V + \mu_V) I_V\right]. \end{aligned}$$

We now obtained the following;

$$\begin{aligned} S_{Hn}(t) &= S_{H0} + \tfrac{1}{\Gamma(\vartheta)} \int_0^t (t - \lambda)^{\vartheta - 1} Z_1\left(\lambda, S_{H(n-1)}(\lambda)\right) d\lambda, \\ E_{Hn}(t) &= E_{H0} + \frac{1}{\Gamma(\vartheta)} \int_0^t (t - \lambda)^{\vartheta - 1} Z_2\left(\lambda, \mathrm{E}_{H(n-1)}(\lambda)\right) \mathrm{d}\lambda, \\ I_{Hn}(t) &= I_{H0} + \tfrac{1}{\Gamma(\vartheta)} \int_0^t (t - \lambda)^{\vartheta - 1} Z_3\left(\lambda, I_{H(n-1)}(\lambda)\right) d\lambda, \quad (16) \\ T_{Hn}(t) &= T_{H0} + \frac{1}{\Gamma(\vartheta)} \int_0^t (t - \lambda)^{\vartheta - 1} Z_4\left(\lambda, \mathrm{T}_{H(n-1)}(\lambda)\right) \mathrm{d}\lambda, \\ V_{Hn}(t) &= V_{H0} + \tfrac{1}{\Gamma(\vartheta)} \int_0^t (t - \lambda)^{\vartheta - 1} Z_5\left(\lambda, V_{H(n-1)}(\lambda)\right) d\lambda, \\ R_{Hn}(t) &= R_{H0} + \tfrac{1}{\Gamma(\vartheta)} \int_0^t (t - \lambda)^{\vartheta - 1} Z_6\left(\lambda, R_{H(n-1)}(\lambda)\right) d\lambda, \\ S_{Vn}(t) &= S_{V0} + \tfrac{1}{\Gamma(\vartheta)} \int_0^t (t - \lambda)^{\vartheta - 1} Z_7\left(\lambda, S_{V(n-1)}(\lambda)\right) d\lambda, \\ I_{Vn}(t) &= I_{V0} + \tfrac{1}{\Gamma(\vartheta)} \int_0^t (t - \lambda)^{\vartheta - 1} Z_8\left(\lambda, I_{V(n-1)}(\lambda)\right) d\lambda. \end{aligned}$$

Transforming equation eq. (13) to get

$$X(t) = X(0) + \tfrac{1}{\Gamma(\vartheta)} \int_0^t (t - \lambda)^{\vartheta - 1} Z\left(\lambda, X(\lambda)\right) d\lambda. \quad (17)$$

Lemma 1, The Lipchitz condition described from Eq. (14) is satisfied by vector $Z(t, D(t))$ on a set $[0, V[]_+^8]$ with the Lipchitz constant given as:

$$\psi = max\left(\left(b\beta_H^* + \beta_V^* + \sigma_2 + \mu_H\right), (\alpha + \mu_h), (\theta + \delta + \mu_h), (\omega + \phi\delta + \mu_H), (\sigma_1 + \mu_H), (\rho + \mu_H), \mu_V, (\delta_V + \mu_V)\right).$$

Proof.

$\|Z_1(t,S_H) - Z_1(t,S_{H1})\|,$
$= \left\|\Lambda_H + \rho R_H + \sigma_1 V_H - \frac{b\beta_H I_V}{N_H} S_H - (\sigma_2 + \mu_H)S_H - \Lambda_H + \rho R_H + \sigma_1 V_H - \frac{b\beta_H I_V}{N_H} S_H - (\sigma_2 + \mu_H)S_{H1}\right\|,$
$= \left\|-\Lambda_H + \rho R_H + \sigma_1 V_H - \frac{b\beta_H I_V}{N_H} S_H - (\sigma_2 + \mu_H)S_H - \mu_H(S_H - S_{H_1}) + \mu_H(S_H - S_{H_1})\right\| \leq (b\beta_H^* + \beta_V^* + \sigma_2 + \mu_H)\|S_H - S_{H1}\| + \mu_H\|S_H - S_{H1}\| \therefore \|Z_1(t,S_H) - Z_1(t,S_{H1})\| \leq (b\beta_H^* + \beta_V^* + \sigma_2 + \mu_H)\|S_H - S_{H1}\|,$
Similarly, we obtained the following:

$$\begin{aligned}
&\left\|Z_2(t,\mathrm{E}_H) - Z_2(t,\mathrm{E}_{H1})\right\| \leq (\alpha + \mu_H)\left\|\mathrm{E}_H - \mathrm{E}_{H1}\right\|,\\
&\left\|Z_3(t,\mathrm{I}_H) - Z_3(t,\mathrm{I}_{H1})\right\| \leq (\theta + \delta + \mu_h)\left\|\mathrm{I}_H - \mathrm{I}_{H1}\right\|,\\
&\|Z_4(t,T_H\ \ ) - Z_4(t,T_{H1}\ \ )\| \leq (\omega + \phi\delta + \mu_H)\|T_H - T_{H1}\ \ \|,\\
&\|Z_5(t,V_H\ \ ) - Z_5(t,V_{H1}\ \ )\| \leq (\sigma_1 + \mu_H)\|V_H - V_{H1}\|,\\
&\|Z_6(t,R_H\ \ ) - Z_6(t,R_{H1}\ \ )\| \leq (\rho + \mu_H)\|R_H - R_{H1}\|,\\
&\|Z_7(t,S_V) - Z_7(t,S_{V1})\| \leq (\mu_V)\|S_V - S_{V1}\|,\\
&\|Z_8(t,I_V\ \ ) - Z_8(t,I_{V1}\ \ )\| \leq (\delta_V + \mu_V)\|I_V - I_{V1}\|.
\end{aligned} \tag{18}$$

Where we obtained:
$\|Z(t,D_1(t)) - Z(t,D_2(t))\| \leq \psi\|D_1 - D_2\|,$
$\psi = max\left((b\beta_H^* + \beta_V^* + \sigma_2 + \mu_H), (\alpha + \mu_h), (\theta + \delta + \mu_h), (\omega + \phi\delta + \mu_H), (\sigma_1 + \mu_H), (\rho + \mu_H), \mu_V, (\delta_V + \mu_V)\right).$ (19)

Lemma 2. The initial value problem (6), (7) in Eq. (19) exists and will have a unique solution $D(t) \in D_c^0(E)$.
Using Picard Lindelöf and fixed-point theory, we consider the solution of
$D(t) = S_H(D(t)),$
where S is defined as the Picard operator expressed as ;
$S_H: D_c^0(E, R_+^8) \to D_c^0(E, R_+^8).$
Therefore
$S_H(D(t)) = D(0) + \frac{1}{\Gamma(\vartheta)}\int_0^t (t-\lambda)^{\vartheta-1} Z(\lambda, D(\lambda))\, d\lambda.$
which becomes:
$\|S_H(D_1(t)) - S_H(D_2(t))\|,$
$= \left\|\frac{1}{\Gamma(\vartheta)}\left[\int_0^t (t-\lambda)^{\vartheta-1} Z(\lambda, D_1(\lambda)) - Z(\lambda, D_2(\lambda))\, d\lambda\right]\right\|,$
$\leq \frac{1}{\Gamma(\vartheta)}\int_0^t (t-\lambda)^{\vartheta-1}\, \|Z(\lambda, D_1(\lambda)) - Z(\lambda, D_2(\lambda))\, d\lambda\|.$
$\leq \frac{\psi}{\Gamma(\vartheta)}\int_0^t (t-\lambda)^{\vartheta-1}\, \|D_1 - D_2\| d\lambda.$
$\|S_H(D_1(t)) - S_H(D_2(t))\| \leq \frac{\psi}{\Gamma(\vartheta+1)S_H}.$
When $\frac{\psi}{\Gamma(\vartheta+1)} S_H \leq 1.$ (20)
then the Picard operator gives a contradiction , so Eq.(6) , (7) solution is unique.

Disease Free Equilibrium Point
Disease free equilibrium point is a point where there is no disease in the population
At DFE $S_H \neq 0, E_H = 0, I_H = 0, T_H = 0, V_H \neq 0, R_H = 0, S_V \neq 0, I_V = 0.$
$(S_H^0, E_H^0, I_H^0, T_H^0, V_H^0, R_H^0, S_V^0, I_V^0\ \ ) = \left(\frac{\Lambda_H(\sigma_1+\mu_H)}{\mu_H(\sigma_2+\sigma_1+\mu_H)}, 0,0,0, \frac{\sigma_2\Lambda_H}{\mu_H(\sigma_2+\sigma_1+\mu_H)}, 0, \frac{\Lambda_V}{\mu_V}, 0\right).$ (21)

Basic Reproduction Number
Basic reproduction number R_0^D:represents the average number of secondary infections caused by a single infected person. To compute R_0^D, we use the next-generation method specifically, by working with a non-negative matrix F (which contains the new infection terms) and another matrix *V* (which covers all other transitions between compartments). The value of R_0^D is then given by the dominant eigenvalue$R_0^D = \rho FV^{-1}$.

$$F=\begin{pmatrix}0 & 0 & 0 & \frac{b\beta_H(\sigma_1+\mu_H)}{\sigma_2+\sigma_1+\mu_H}\\ 0 & 0 & 0 & 0\\ 0 & 0 & 0 & 0\\ 0 & \frac{\beta_V\Lambda_V\mu_H}{\Lambda_V\mu_V} & 0 & 0\end{pmatrix} V=\begin{pmatrix}G_2 & 0 & 0 & 0\\ -\alpha & G_3 & 0 & 0\\ 0 & -\theta & G_4 & 0\\ 0 & 0 & 0 & G_8\end{pmatrix} \quad (22)$$

$$V^{-1}=\begin{pmatrix}\frac{1}{G_2} & 0 & 0 & 0\\ \frac{\alpha}{G_2G_3} & \frac{1}{G_3} & 0 & 0\\ \frac{\theta\alpha}{G_2G_3G_4} & \frac{\theta}{G_3G_4} & \frac{1}{G_4} & 0\\ 0 & 0 & 0 & \frac{1}{G_8}\end{pmatrix},$$

$$FV^{-1}=\begin{pmatrix}0 & 0 & 0 & \frac{b\beta_H(\sigma_1+\mu_H)}{(\sigma_2+\sigma_1+\mu_H)G_8}\\ 0 & 0 & 0 & 0\\ 0 & 0 & 0 & 0\\ \frac{\beta_V\Lambda_V\mu_H\alpha}{\Lambda_H\mu_VG_2G_3} & \frac{\beta_V\Lambda_V\mu_H}{\Lambda_H\mu_VG_3} & 0 & 0\end{pmatrix},$$

$$R_0^D=\frac{\sqrt{\Lambda_H\mu_vG_2G_3(\sigma_2+\sigma_1+\mu_H)G_8\beta_v\Lambda_v\mu_H\alpha b\beta_H(\sigma_1+\mu_H)}}{\Lambda_H\mu_vG_2G_3(\sigma_2+\sigma_1+\mu_H)G_8}. \quad (23)$$

Where$G_1=(\sigma_2+\mu_H), G_2=(\alpha+\mu_h), G_3=(\theta+\delta+\mu_h), G_4=(\omega+\phi\delta+\mu_H),$
$G_5=(\sigma_1+\mu_H), G_6=(\rho+\mu_H), G_7=\mu_V, G_8=(\delta_V+\mu_V).$

Endemic Equilibrium Point

The endemic equilibrium represents a state in which Dengue fever persists continuously within the human population over time.

At endemic equilibrium point $S_H\neq 0, E_H\neq 0, I_H\neq 0, T_H\neq 0, V_H\neq 0, R_H\neq 0, S_V\neq 0, I_V\neq 0.$

We obtain the following endemic equilibrium points:

$$S_H^{**}=-\frac{\Lambda_HG_2G_3G_4G_5G_6}{((-\lambda_H-G_1)G_5+\sigma_1\sigma_2)G_3G_4G_6G_2+\alpha\omega\rho\theta G_5\lambda_H},$$
$$E_H^{**}=-\frac{\Lambda_HG_3G_4G_5G_6\lambda_H}{((-\lambda_H-G_1)G_5+\sigma_1\sigma_2)G_3G_4G_6G_2+\alpha\omega\rho\theta G_5\lambda_H},$$
$$I_H^{**}=-\frac{\alpha\Lambda_HG_4G_5G_6\lambda_H}{((-\lambda_H-G_1)G_5+\sigma_1\sigma_2)G_3G_4G_6G_2+\alpha\omega\rho\theta G_5\lambda_H},$$
$$T_H^{**}=-\frac{\alpha\Lambda_HG_5G_6\lambda_H\theta}{((-\lambda_H-G_1)G_5+\sigma_1\sigma_2)G_3G_4G_6G_2+\alpha\omega\rho\theta G_5\lambda_H}, \quad (24)$$
$$V_H^{**}=-\frac{\Lambda_HG_2G_3G_4G_6\sigma_2}{((-\lambda_H-G_1)G_5+\sigma_1\sigma_2)G_3G_4G_6G_2+\alpha\omega\rho\theta G_5\lambda_H},$$
$$R_H^{**}=-\frac{\theta\lambda_HG_5\Lambda_H\omega\alpha}{\alpha\omega\rho\theta G_5\lambda_H-G_1G_2G_3G_4G_5G_6-G_2G_3G_4G_5G_6\lambda_H+G_2G_3G_4G_6\sigma_1\sigma_2},$$
$$S_V^{**}=\frac{\Lambda_V\begin{pmatrix}\alpha\omega\theta G_5\lambda_H+\alpha\theta G_5G_6\lambda_H+\alpha G_4G_5G_6\lambda_H+G_2G_3G_4G_5G_6\\ +G_2G_3G_4G_6\sigma_2+G_3G_4G_5G_6\lambda_H\end{pmatrix}}{\begin{matrix}\alpha\omega\theta G_5G_7\lambda_H+\alpha\theta G_5G_6G_7\lambda_H+\alpha G_4G_5G_6G_7\lambda_H+\beta_V\alpha G_4G_5G_6\lambda_H\\ +G_2G_3G_4G_5G_6G_7+G_2G_3G_4G_6G_7\sigma_2+G_3G_4G_5G_6G_7\lambda_H\end{matrix}},$$

$$I_V^{**}=\frac{G_4G_5G_6\beta_V\lambda_H\alpha\Lambda_V}{G_8\begin{pmatrix}\alpha\omega\theta G_5G_7\lambda_H+\alpha\theta G_5G_6G_7\lambda_H+\alpha G_4G_5G_6G_7\lambda_H+\beta_V\alpha G_4G_5G_6\lambda_H\\ +G_2G_3G_4G_5G_6G_7+G_2G_3G_4G_6G_7\sigma_2+G_3G_4G_5G_6G_7\lambda_H\end{pmatrix}}.$$

Substituting into the force of infections: $\lambda_H=\frac{b\beta_HI_V}{N_H}$and $\lambda_V=\frac{\beta_VI_H}{N_H}$.

We have:

$P_1\lambda_H^2+P_2\lambda_2+P_3=0.$

Where

$$P_1=\begin{pmatrix}\alpha^2\omega^2\theta^2{G_5}^2G_7G_8+2\alpha^2\omega\theta^2{G_5}^2G_6G_7G_8+2\alpha^2\omega\theta G_4{G_5}^2G_6G_7G_8\\ +\alpha^2\omega\theta G_4{G_5}^2G_6G_8\beta_V+\alpha^2\theta^2{G_5}^2{G_6}^2G_7G_8+2\alpha^2\theta G_4{G_5}^2{G_6}^2G_7G_8\\ +\alpha^2\theta G_4{G_5}^2{G_6}^2G_8\beta_V+\alpha^2{G_4}^2{G_5}^2{G_6}^2G_7G_8+\alpha^2{G_4}^2{G_5}^2{G_6}^2G_8\beta_V\\ +2\alpha G_3{G_4}^2{G_5}^2{G_6}^2G_7G_8{\lambda_H}^2+2\alpha\omega\theta G_3G_4{G_5}^2G_6G_7G_8\\ +2\alpha\theta G_3G_4{G_5}^2{G_6}^2G_7G_8+\alpha G_3{G_4}^2{G_5}^2{G_6}^2G_8\beta_V+{G_3}^2{G_4}^2{G_5}^2{G_6}^2G_7G_8\end{pmatrix},$$

$$P_2 = \begin{pmatrix} 2\alpha\omega\theta G_2 G_3 G_4 {G_5}^2 G_6 G_7 G_8 \lambda_H + 2\alpha\omega\theta G_2 G_3 G_4 G_5 G_6 G_7 G_8 \lambda_H \sigma_2 \\ +2\alpha\theta G_2 G_3 G_4 {G_5}^2 {G_6}^2 G_7 G_8 \lambda_H + 2\alpha\theta G_2 G_3 G_4 G_5 {G_6}^2 G_7 G_8 \lambda_H \sigma_2 \\ +2\alpha\theta G_3 G_4 {G_5}^2 {G_6}^2 G_7 G_8 {\lambda_H}^2 + 2\alpha G_2 G_3 {G_4}^2 {G_5}^2 {G_6}^2 G_7 G_8 \lambda_H \\ +\alpha G_2 G_3 {G_4}^2 {G_5}^2 {G_6}^2 G_8 \beta_V \lambda_H + 2\alpha G_2 G_3 {G_4}^2 G_5 {G_6}^2 G_7 G_8 \lambda_H \sigma_2 \\ +\alpha G_2 G_3 {G_4}^2 G_5 {G_6}^2 G_8 \beta_V \lambda_H \sigma_2 + 2 G_2 G_3 {G_3}^2 {G_4}^2 {G_5}^2 {G_6}^2 G_7 G_8 \lambda_H \\ +2 G_2 G_3 {G_3}^2 {G_4}^2 G_5 {G_6}^2 G_7 G_8 \lambda_H \sigma_2 \end{pmatrix},$$

$$P_3 = G_1 G_2 (1 - (R_0^D)^2). \quad (25)$$

The endemic equilibrium points are obtained from solving for λ_H^{**} in the polynomial, and substituting the positive values of λ_V^{**} into the expression λ_H^{**}, Furthermore, it follows that the coefficient is always positive , and is positive (negative) if R_0^D is less (greater) than one.

Fractional order model numerical results

To solve the fractional-order Dengue fever model numerically, we used the generalized fractional Adams-Bashforth-Moulton method developed by Amos et al. (2024). The parameter values we used in the simulation are listed in Table 2, which also shows the different fractional-order values(ϑ) we tested.

Implementation of fractional Adams–Bashforth–Moulton method

The method described by Jalija et al. (2026) has been applied in this study. Using the fractional Adams-Bashforth-Moulton method, we derived an approximate solution for the fractional Dengue fever model presented in equation (6). The fractional model (6) is now ${}^{c}D_t^{\vartheta} H(t) = Q(t, q(t)), 0 < t < \vartheta,$ (26)

$H^{(n)}(0) = H_0^{(n)}, n = 1,0, \ldots, q, q = [\kappa].$

Where $H = \left(S_H^*, E_H^*, I_H^*, T_H^*, V_H^*, R_Z^* S_V^*, I_V^* \right) \in R_+^8$ and $W(t, q(t))$ is a real valued function that is continuous. Eq. (27) can be therefore be represented using the concept of fractional integral as follows;

$$H(t) = \sum_{n=0}^{m-1} H_0^{(n)} \frac{t^n}{n!} + \frac{1}{\Gamma(\vartheta)} \int_0^t (t-y)^{\vartheta - 1} R\big(k, m(k)\big) dk \quad (27)$$

Using the method described by Amos et al.(2024), we let the step size $g = \frac{\vartheta}{N}, N \in N$ with a grid that is uniform on $[0, \vartheta]$. Where $t_c = cr, c = 0,1,1, \ldots N$. Therefore, and the fractional order model of Dengue fever model presented in (6) can be approximated as:

$$\begin{aligned}
S_{H(k+1)}(t) &= S_{H0} + \frac{g^{\vartheta}}{\Gamma(\vartheta+2)} \left\{ \Lambda_H + \rho R_H^n + \sigma_1 V_H^n - \frac{b\beta_H I_V^n}{N_H^n} S_H^n - (\sigma_2 + \mu_H) S_H^n \right\} + \frac{g^{\vartheta}}{\Gamma(\vartheta+2)} \sum_{y=0}^{k} dy, k+1 \left\{ \Lambda_H + \rho R_{Hy} + \sigma_1 V_{Hy} - \right. \\
&\left. \frac{b\beta_H I_{Vy}}{N_{Hy}} S_{Hy} - (\sigma_2 + \mu_H) S_{Hy} \right\}, \\
E_{H(k+1)}(t) &= E_{H0} + \frac{g^{\vartheta}}{\Gamma(\vartheta+2)} \left\{ \frac{b\beta_H I_V^n}{N_H} S_H^n - (\alpha + \mu_H) E_H^n \right\} + \frac{g^{\vartheta}}{\Gamma(\vartheta+2)} \sum_{y=0}^{k} dy, k+1 \left\{ \frac{b\beta_H I_{Vy}}{N_{Hy}} S_{Hy} - (\alpha + \mu_H) E_{Hy} \right\}, \\
I_{H(k+1)}(t) &= I_{H0} + \frac{g^{\vartheta}}{\Gamma(\vartheta+2)} \{ \alpha E_H^n - (\theta + \delta + \mu_H) I_H^n \} + \frac{g^{\vartheta}}{\Gamma(\vartheta+2)} \sum_{y=0}^{k} dy, k+1 \{ \alpha E_{Hy} - (\theta + \delta + \mu_H) I_{Hy} \}, \\
T_{H(k+1)}(t) &= T_{H0} + \frac{g^{\vartheta}}{\Gamma(\vartheta+2)} \{ \theta I_H^n - (\omega + \phi\delta + \mu_H) T_H^n \} + \frac{g^{\vartheta}}{\Gamma(\vartheta+2)} \sum_{y=0}^{k} dy, k+1 \{ \theta I_{Hy} - (\omega + \phi\delta + \mu_H) T_{Hy} \}, \quad (28) \\
V_{H(k+1)}(t) &= V_{H0} + \frac{g^{\vartheta}}{\Gamma(\vartheta+2)} \{ \sigma_2 S_H^n - (\sigma_1 + \mu_H) V_H^n \} + \frac{g^{\vartheta}}{\Gamma(\vartheta+2)} \sum_{y=0}^{k} dy, k+1 \{ \sigma_2 S_{Hy} - (\sigma_1 + \mu_H) V_{Hy} \}, \\
R_{H(k+1)}(t) &= R_{H0} + \frac{g^{\vartheta}}{\Gamma(\vartheta+2)} \{ \omega T_H^n - (\rho + \mu_H) R_H^n \} + \frac{g^{\vartheta}}{\Gamma(\vartheta+2)} \sum_{y=0}^{k} dy, k+1 \{ \omega T_{Hy} - (\rho + \mu_H) R_{Hy} \}, \\
S_{V(k+1)}(t) &= S_{V0} + \frac{g^{\vartheta}}{\Gamma(\vartheta+2)} \left\{ \Lambda_V - \frac{\beta_V I_H^n}{N_H^n} S_V^n - \mu_V S_V^n \right\} + \frac{g^{\vartheta}}{\Gamma(\vartheta+2)} \sum_{y=0}^{k} dy, k+1 \left\{ \Lambda_V - \frac{\beta_V I_{Hy}}{N_H} S_{Vy} - \mu_V S_{Vy} \right\}, \\
I_{V(k+1)}(t) &= I_{V0} + \frac{g^{\vartheta}}{\Gamma(\vartheta+2)} \left\{ \frac{\beta_V I_H^n}{N_H^n} S_V^n - (\delta_V + \mu_V) I_V^n \right\} + \frac{g^{\vartheta}}{\Gamma(\vartheta+2)} \sum_{y=0}^{k} dy, k+1 \left\{ \frac{\beta_V I_{Hy}}{N_H} S_{Vy} - (\delta_V + \mu_V) I_{Vy} \right\}.
\end{aligned}$$

Where

$$\begin{aligned}
S_{H(k+1)}^n(t) &= S_{H0} + \frac{1}{\Gamma(\vartheta)} \sum_{y=0}^{k} f_{y,k+1} \left\{ \Lambda_H + \rho R_{Hy} + \sigma_1 V_{Hy} - \frac{b\beta_H I_{Vy}}{N_{Hy}} S_{Hy} - (\sigma_2 + \mu_H) S_{Hy} \right\}, \\
E_{H(k+1)}^n(t) &= E_{H0} + \frac{1}{\Gamma(\vartheta)} \sum_{y=0}^{k} f_{y,k+1} \left\{ \frac{b\beta_H I_{Vy}}{N_{Hy}} S_{Hy} - (\alpha + \mu_H) E_{Hy} \right\}, \\
I_{H(k+1)}^n(t) &= I_{H0} + \frac{1}{\Gamma(\vartheta)} \sum_{y=0}^{k} f_{y,k+1} \{ \alpha E_{Hy} - (\theta + \delta + \mu_H) I_{Hy} \}, \\
T_{H(k+1)}^n(t) &= T_{H0} + \frac{1}{\Gamma(\vartheta)} \sum_{y=0}^{k} f_{y,k+1} \{ \theta I_{Hy} - (\omega + \phi\delta + \mu_H) T_{Hy} \}, \\
V_{H(k+1)}^n(t) &= V_{H0} + \frac{1}{\Gamma(\vartheta)} \sum_{y=0}^{k} f_{y,k+1} \{ \sigma_2 S_{Hy} - (\sigma_1 + \mu_H) V_{Hy} \}, \quad (29) \\
R_{H(k+1)}^n(t) &= R_{H0} + \frac{1}{\Gamma(\vartheta)} \sum_{y=0}^{k} f_{y,k+1} \{ \omega T_{Hy} - (\rho + \mu_H) R_{Hy} \},
\end{aligned}$$

$S^n_{V(k+1)}(t) = S_{V0} + \frac{1}{\Gamma(\vartheta)}\sum_{y=0}^{k} f_{y,k+1}\left\{\Lambda_V - \frac{\beta_V I_{Hy}}{N_H} S_{Vy} - \mu_V S_{Vy}\right\},$

$I^n_{V(k+1)}(t) = I_{V0} + \frac{1}{\Gamma(\vartheta)}\sum_{y=0}^{k} f_{y,k+1}\left\{\frac{\beta_V I_{Hy}}{N_H} S_{Vy} - (\delta_V + \mu_V) I_{Vy}\right\}.$

From (29) and (30) obtained:

$dy_{,K+1} = K^{\vartheta+1} - (k-\vartheta)(k+\vartheta)^{\vartheta}, y = 0.$

$(k-y+2)^{\vartheta+1} + (k-\vartheta)^{\vartheta+1} - 2(k-y+1)^{\vartheta+1}, 1 \le y \le k$

and $f_{y,k+1} = \frac{g^{\vartheta}}{\vartheta}\left[(k-y+1)^{\vartheta}(k-y)^{\vartheta}\right], 0 \le y \le k.$

Importance of using the fractional Adam-Bashforth Moulton method in obtaining the numerical solutions of the model

1. The fractional Adams-Bashforth-Moulton method requires only one extra function evaluation per step and retains the high-order accuracy.
2. This method has error control and is widely used for integration in ODE solvers.
3. This method is a powerful tool for numerical solution of partial and fractional-order differential equations and has wide applications in engineering, chemistry, medicine, etc.

Table 2: Table of parameter values used for Numerical Simulation

Parameters	Values	Sources
Λ_h	500	Garba et al. (2008)
Λ_V	10,000,000	Garba et al. (2008)
μ_H	0.02041	Samir et al.(2013)
μ_V	0.5	Samir et al.(2013)
β_H	0.5	Garba et al. (2008)
β_V	0.4	Garba et al. (2008)
ρ	0.1	Garba et al. (2008)
ω	0.3254	Garba et al. (2008)
δ	0.365	Samir et al.(2013)
δ_V	0.21	Assumed
α	0.3	Jalija et al.(2025)
θ	0.5	Assumed
σ_1	0.03	Assumed
σ_2	0.5	Jalija et al.(2025)
ϕ	0.5	Assumed

RESULTS AND DISCUSSION

Numerical simulation

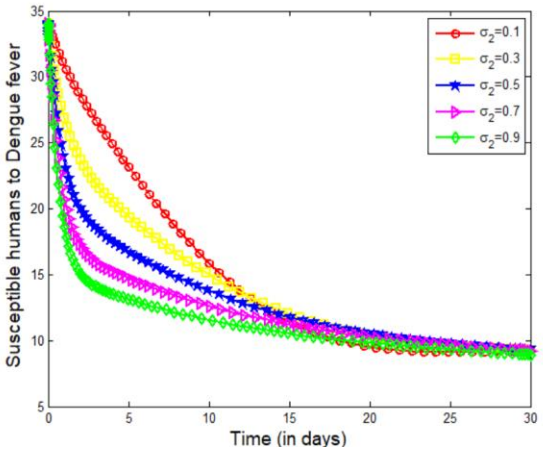

Figure 2a: Simulation of the effect of σ_2 on susceptible human population

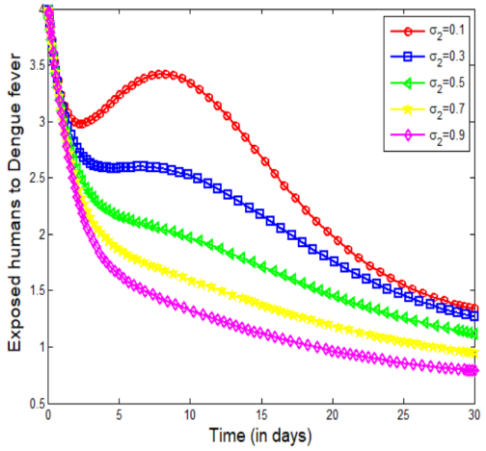

Figure 2b: Simulation of the effect of σ_2 on exposed human population

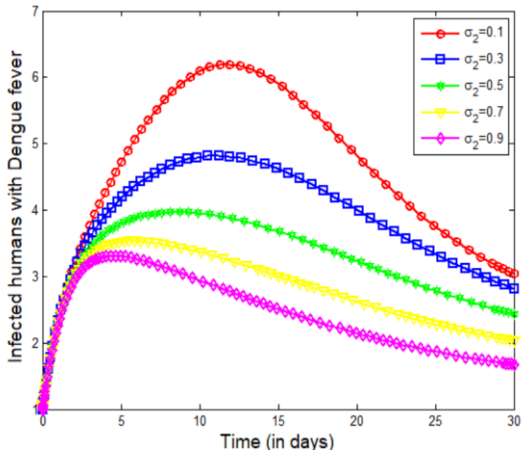

Figure 2c: Simulation of the effect of σ_2 on infected human population

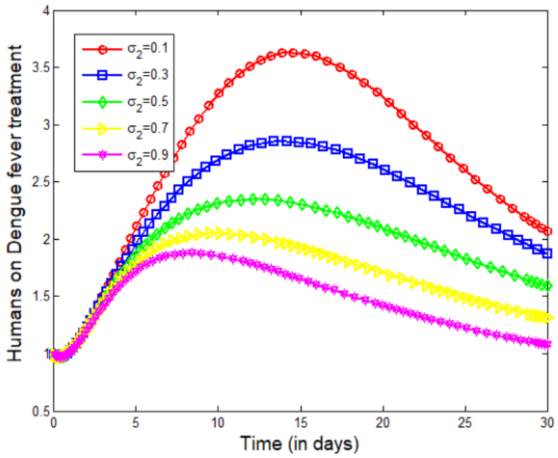

Figure 2d: Simulation of the effect of σ_2 on human population on treatment

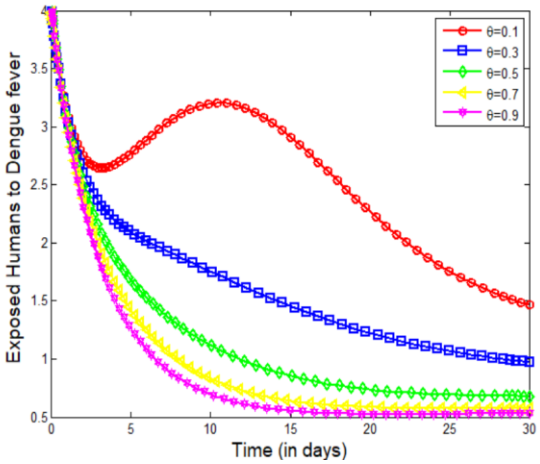

Figure 2e: Simulation of the effect of θ on exposed human population

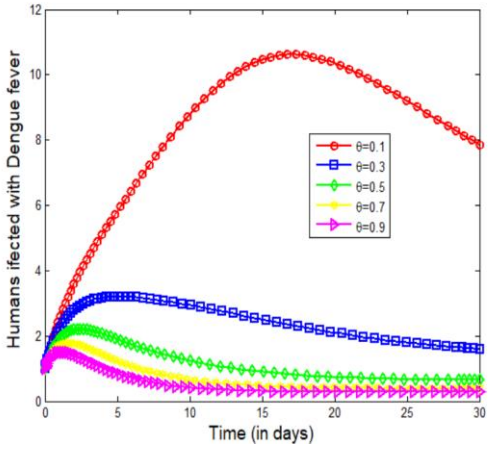

Figure 2f: Simulation of the effect of θ on infected human population

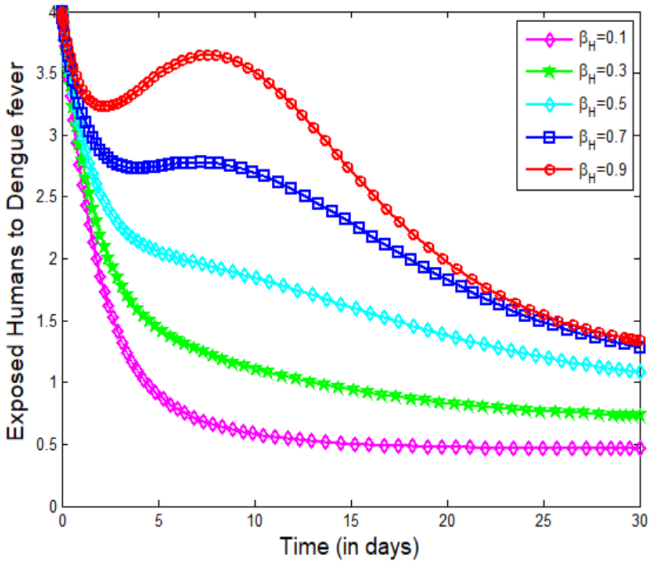

Figure 2g: Simulation of the effect of β_H on exposed human population

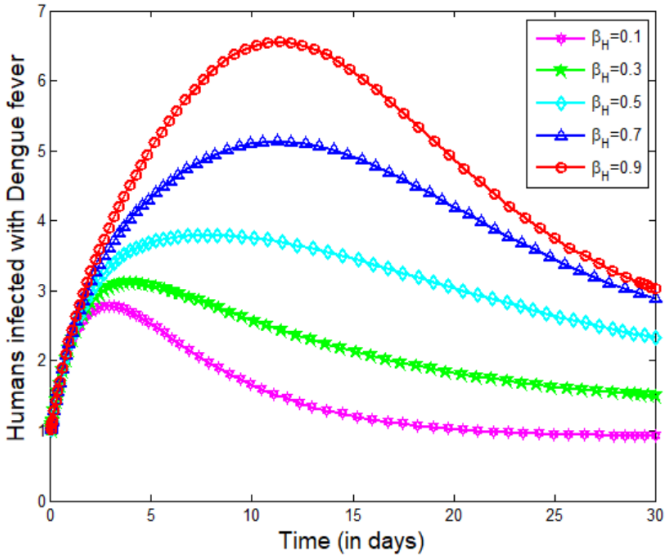

Figure 2h: Simulation of the effect of β_H on infected human population

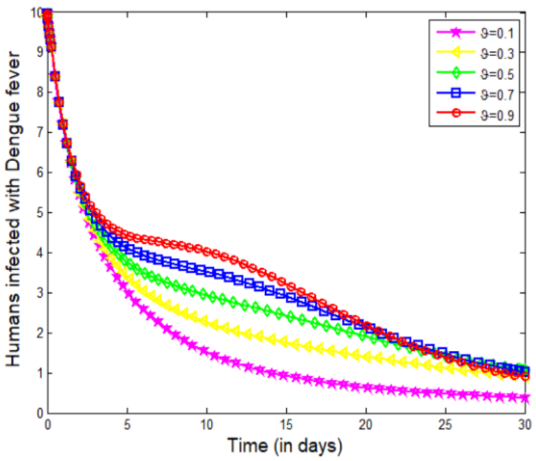

Figure 2i: Simulation of the effect of ϑ on infected human population

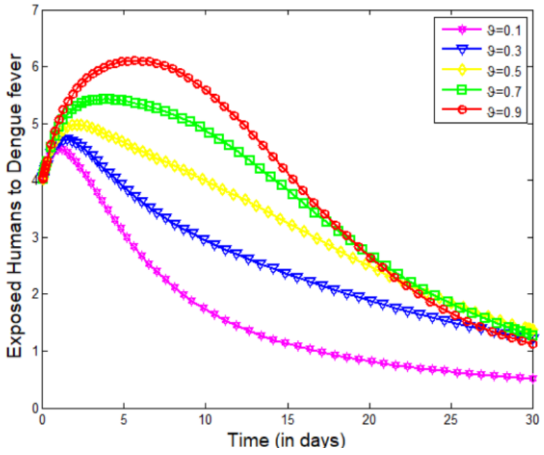

Figure 2j: Simulation of the effect of ϑ on exposed human population

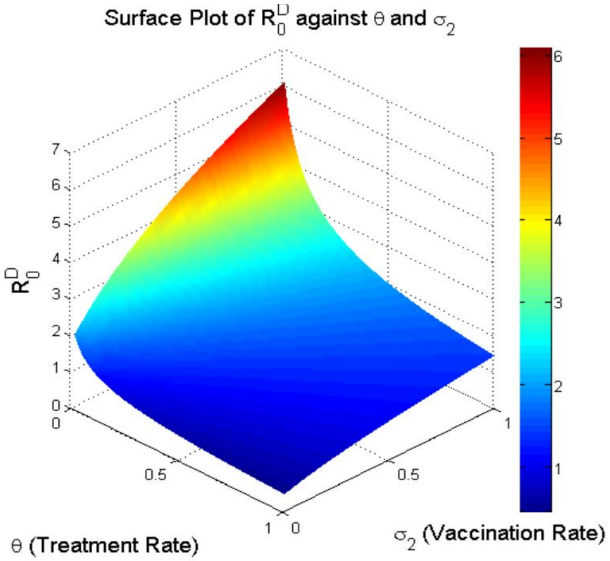

Figure 2k: Surface plot showing the effect of σ_2 and θon R_0^D

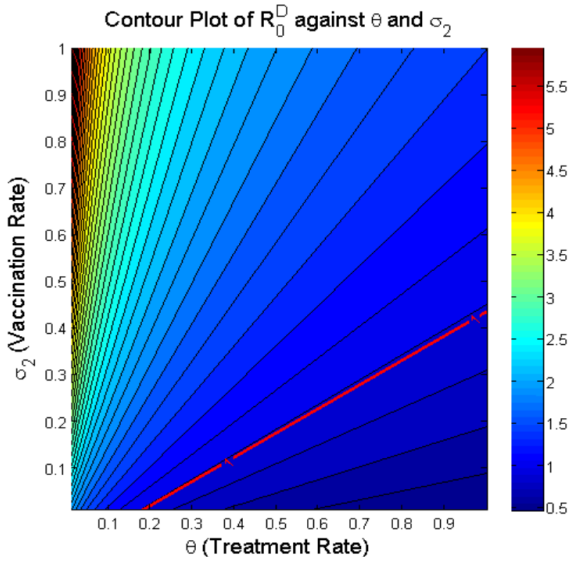

Figure 2l: Contour plot showing the effect of σ_2 and θon R_0^D

Figure 2a, shows how the vaccination rate $\sigma_2$affects the number of people susceptible to Dengue fever. The higher the vaccination rateσ_2, the faster the susceptible population drops over time. Figure 2b shows the impact on the exposed population. As the vaccination rate $\sigma_2$goes up, the number of exposed individuals falls sharply as time goes on. In Figure 2c, we observe a similar trend for infected people. A higher vaccination rate $\sigma_2$leads to a clear and significant decline in the infected population over time. Figure 2d illustrates what happens to those receiving treatment for Dengue. As vaccination coverage σ_2 increases, fewer people end up needing treatment, and the treated population steadily decreases over time. Figure 2e looks at how the treatment θ rate influences the number of people exposed to Dengue fever. As treatment ratesθ rise, the exposed population drops noticeably over time. In Figure 2f, we turn to the infected population. The pattern is similar: with higher treatment ratesθ, the number of infected individuals falls significantly as time goes on. Figure 2g explores the role of the contact rate β_H. Unsurprisingly, when contact rates β_H increase, the exposed population grows substantially over time. Figure 2h shows the effect on infected individuals. As the contact rate β_H goes up, the infected population also rises sharply over the course of the simulation. Figure (2i) looks at how the fractional order ϑaffects the number of people exposed to Dengue fever. As the fractional order ϑincreases, the exposed population grows significantly over time. Similarly, Figure (2j) shows the impact on infected individuals. When the fractional order ϑgoes up, the infected population also rises sharply as time progresses. Figure (2k), illustrates the shape of the relationship between θ and σ_2 on R_0^D. The curve shows that the maximum value reached is 0.8, and the key parameter remains below one (1). This suggests that even if we push θ and $\sigma_2$further, they probably won't cause a major spike in Dengue infections. Finally, (2l) reveals something more encouraging: when θ and $\sigma_2$increase, the basic

reproduction number R_0^D drops below one much earlier. This means that boosting θ and $\sigma_2$can eventually help reduce the overall impact of Dengue fever on the human population.

CONCLUSION

Finally, the fractional order mathematical model obtained in this study has given a better understanding of transmission dynamics and control mechanisms of Dengue fever in a susceptible population. By introducing the FD, the model provides a more realistic description of the disease dynamics since it reflects memory effects and the hereditary nature of the disease transmission process. The analytical and numerical studies showed that disease control and possible elimination are improved when effective vaccination and treatment policies reduce the basic reproduction number to less than unity. The study also confirmed that the enhanced effective contact rates between susceptible and infected vectors play significant roles in the persistence and fast propagation of Dengue fever in the population. The numerical simulation showed that reducing vector-human interactions, making treatment accessible, and increasing vaccination coverage are essential to reduce the prevalence and mortality due to Dengue infection. Furthermore, the numerical simulation results verified that the proposed model is stable and reliable for different fractional-order operators, suggesting that fractional calculus is a useful tool for handling complex epidemiological systems. The findings further highlight the need for both pharmaceutical and non-pharmaceutical interventions, such as vector control, environmental sanitation, public health awareness campaigns, early diagnosis, and prompt medical treatment, as crucial tools in the fight against Dengue fever outbreaks. Hence, for a successful control and eventual elimination of Dengue fever, particularly in endemic areas, continuous endeavours by the government and public health agencies towards immunization programmes, effective vector control measures, development of an improved health delivery system, and the continuous creation of public awareness are highly recommended. Finally, the developed model can provide a useful mathematical framework for future studies on Dengue fever and other vector-borne infectious diseases based on fractional order models.

REFERENCES

Abah, E., Bolaji, B., Atokolo, W., Amos, J., Acheneje, G. O., Omede, B. I., Omeje, D. (2024). Fractional mathematical model for the transmission dynamics and control of diphtheria. *International Journal of Mathematical Analysis and Modelling*, 7, ISSN: 2682-5694.

Abro, K., Atangana, A., & Gómez-Aguilar, J. F. (2021). An analytic study of bioheat transfer Pennes model via modern non-integer differential techniques. *European Physical Journal Plus*, 136. https://doi.org/10.1140/epjp/s13360-021-02136-x

Agahiu, N., Bolaji, B., Acheneje, G. O., & Atokolo, W. (2024). Approximate solution of fractional order mathematical model on the co-transmission of Zika and Chikungunya virus using Laplace-Adomian decomposition method. *International Journal of Mathematics*, 7(3), 47–81.

Ahmed, I., Goufo, E. F. D., Yusuf, A., Kumam, P., Chaipanya, P., & Nonlaopon, K. (2021). An epidemic prediction from analysis of a combined HIV-COVID-19 co-infection model via ABC fractional operator. *Alexandria Engineering Journal*, 60(3), 2979–2995.

Ali, Z., Zada, A., & Shah, K. (2017). Existence and stability analysis of three-point boundary value problem. *International Journal of Applied and Computational Mathematics*, 3, 651–664. https://doi.org/10.1007/s40819-017-0375-8

Ameh, P. O., Omede, B. I., & Bolaji, B. (2020). Dynamical analysis of a two-strain treatment model for anthrax in a population where it is deployed as a bioterrorism weapon. *Journal of the Nigerian Society for Mathematical Biology*, 3, 34–77.

Amos, J., Omale, D., Atokolo, W., Abah, E., Omede, B. I., Acheneje, G. O., & Bolaji, B. (2024). Fractional mathematical model for the transmission dynamics and control of Hepatitis C. *FUDMA Journal of Sciences*, 8(5), 451–463. https://doi.org/10.33003/fjs-2024-0805-2883

Atokolo, W. A., Aja, R. O., Omale, D., Ahman, Q. O., Acheneje, G. O., & Amos, J. (2024). Fractional mathematical model for the transmission dynamics and control of Lassa fever. *Journal of Fractional Calculus and Applied Mathematics*. https://doi.org/10.1016/j.fraope.2024.100110

Atokolo, W. A., Aja, R. O., Omale, D., Paul, R. V., Amos, J., & Ocha, S. O. (2023). Mathematical modeling of the spread of vector-borne diseases with influence of vertical transmission and preventive strategies. *FUDMA Journal of Sciences*, 7(6), 75–91. https://doi.org/10.33003/fjs-2023-0706-2174

Atokolo, W., Aja, R. O., Aniaku, S. E., Onah, I. S., & Mbah, G. C. (2022). Approximate solution of the fractional order sterile insect technology model via the Laplace-Adomian decomposition method for the spread of Zika virus disease. *International Journal of Mathematics and Mathematical Sciences*, 2022, Article 2297630.

Baskonus, H. M., & Bulut, H. (2015). On the numerical solutions of some fractional ordinary differential equations by fractional Adams-Bashforth-Moulton method. *Open Mathematics*, 13, 1–9.

Bhatt, S., Gething, P. W., Brady, O. J., Messina, J. P., Farlow, A. W., Moyes, C. L., Drake, J. M., Brownstein, J. S., Hoen, A. G., Sankoh, O., et al. (2013). The global distribution and burden of dengue. *Nature*, 496(7446), 504–507.

Bolaji, B., Ani, F., Omede, B. I., Acheneje, G. O., & Ibrahim, A. (2024). A model for the control of transmission dynamics of human monkeypox disease in sub-Saharan Africa. *Journal of the Nigerian Society of Physical Sciences*, 6, 1800.

Bolaji, B., Odionyenma, U. B., Omede, B. I., Ojih, P., Abdullahi, B., & Ibrahim, A. (2023). Modelling the transmission dynamics of Omicron variant of COVID-19 in densely populated city of Lagos in Nigeria. *Journal of the Nigerian Society of Physical Sciences*, 5, 1055.

Brady, O. J., Gething, P. W., Bhatt, S., Messina, J. P., Brownstein, J. S., Hoen, A. G., Moyes, C. L., Farlow, A. W., Scott, T. W., & Hay, S. I. (2012). Refining the global spatial limits of dengue virus transmission by evidence-based consensus. *PLoS Neglected Tropical Diseases*, 6(8), e1760.

Chen, Y., Wong, K., & Zhao, L. (2023). Modeling the impact of vaccination strategies on hepatitis C and COVID-19 coinfection dynamics. *Journal of Vaccine*, 41(15), 2897–2905.

Chikaki, E., & Ishikawa, H. (2009). A dengue transmission model in Thailand considering sequential infections with all four serotypes. *Journal of Infection in Developing Countries*, 3(9), 711–722.

Das, R., Patel, S., & Kumar, A. (2024). Mathematical modeling of hepatitis C and COVID-19 coinfection in low- and middle-income countries: Challenges and opportunities. *BMC Public Health*, 24(1), 587.

Dengue Virus Net. (2018). Treatment of dengue. Retrieved from http://www.denguevirusnet.com/treatment.html

Dengue Virus Net. (2019). Dengue virus transmission. Retrieved from https://www.denguevirusnet.com/transmission.html

Diethelm, K. (1999). *The Frac PECE subroutine for the numerical solution of differential equations of fractional order*.

Emmanuel, L., Omale, D., Atokolo, W., Amos, J., Abah, E., Ojonimi, A., Onoja, T., Acheneje, G., & Bolaji, B. (2025). Fractional mathematical model for the dynamics of pneumonia transmission with control using fixed point theory. *GPH-International Journal of Mathematics*, 8(5), 55–86. https://doi.org/10.5281/zenodo.16364036

Garba S. M., Gumel .A. B. & Abubakar .M.R., (2008) "Backward Bifurcations in Dengue Transmission Dynamics", Mathematical Biosciences 215 11.

Gubler, D. J. (1998). Dengue and dengue hemorrhagic fever. *Clinical Microbiology Reviews*, 11(3), 480–496.

Halstead, S. B., Nimmannitya, S., & Cohen, S. N. (1970). Observations related to pathogenesis of dengue hemorrhagic fever IV: Relation of disease severity to antibody response and virus recovered. *Yale Journal of Biology and Medicine*, 42(5), 311.

Jalija, E., Amos, J., Atokolo, W., Abah, E., Agbata, B. C., Acheneje, G. O., Shyamsunder, & Bolaji, B. (2026). Numerical solution of fractional order typhoid fever model via the generalized fractional Adams-Bashforth-Moulton approach. *Network Modeling Analysis in Health Informatics and Bioinformatics*, 15, 68. https://doi.org/10.1007/s13721-026-00743-1

Jalija, E., Amos, J., Atokolo, W., Omale, D., Abah, U., Alih, U., Alabi, P. A., & Bolaji, B. (2025). Numerical investigations on dengue fever model through singular and non-singular fractional operators. *International Journal of Mathematical Analysis and Modelling*, 8(1), 216–242.

Odiba, P. O., Acheneje, G. O., & Bolaji, B. (2024). A compartmental deterministic epidemiological model with nonlinear differential equations for analysing the co-infection dynamics between COVID-19, HIV, and monkeypox diseases. *Healthcare Analytics*, 5, 100311. https://doi.org/10.1016/j.health.2024.100311

Ojonimi, A. A., Amos, J., Atokolo, W., Omale, D., Emmanuel, L. M., Abah, E., Acheneje, G. O., & Bolaji, B. (2025). Numerical solution of fractional order Hepatitis B model via the generalized fractional Adams-Bashforth-Moulton approach. *Journal of Science Research and Reviews*, 2(5), 33–48. https://doi.org/10.70882/josrar.2025.v2i5.119

Omale, D., Akpa, M., & Atokolo, W. (2020). Global stability and sensitivity analysis of transmission dynamics of tuberculosis and its control: A case study of Ika General Hospital Ankpa, Kogi State, Nigeria. *Academic Journal of Statistics and Mathematics*, 6.

Omale, D., Atokolo, W., .Akpa, M., (2020). Global stability and sensitivity analysis of transmission dynamics of tuberculosis and its control, A case study of Ika general hospital Ankpa, Kogi State, Nigeria. Acad. J. Stat. Math. 6, 5730-7151.

Omale, D., Ojih, P., Atokolo, W., Omale, A., Bolaji.B. (2021), Mathematical model for transmission dynamics of HIV and Tuberculosis co-infection in Kogi State, Nigeria. Journal of Mathematical Computational Science. 11, No. 5, 5580-5613. Available online at: https://doi.org/10.28919/jmcs/6080.

Omame, A.M., Abbas, M., Onyenegecha, C.P. (2022), "A fractional order model for the co-interaction of COVID-19 and hepatitis B virus." *Journal of Mathematical Biology*, pp. 112–118.

Omede, B. I., Bolarinwa Bolaji, Olumuyiwa, P. J., Ibrahim, A. A. and Oguntolu F. A (2023). Mathematical analysis on the vertical and horizontal transmission dynamics of HIV and Zika virus co-infection. Franklin open 6 100064. https://doi.org/10.1016/j.fraope.2023.100064. - Elsevier Journal .

Omede, B. I., Olumuyiwa, P. J., Atokolo, W., Bolaji, B. & Ayoola, T. A. (2023). A mathematical analysis of the two-strain tuberculosis model dynamics with exogenous re-infection. Healthcare Analytics 4, 100266. https://doi.org/10.1016/j.health.2023.100266 .

Omede, B.I., Israel, M., Mustapha, M. K., Amos, J., Atokolo, W., & Oguntolu, F. A. (2024). "Approximate solution to the fractional soil-transmitted helminth infection model using Laplace-Adomian Decomposition Method," *International Journal of Mathematics*, 07(04), pp. 16–40.

Omonu, G. U., Ameh, P.O., Omede, B.I, & Bolaji.B (2019), Mathematical modelling of Tuta Absoluta on Tomato plants. Journal of the Nigerian Society for Mathematical Biology. 2(1): 14-31.

Philip J., Omale D., Atokolo W., Amos J., Acheneje G.O., Bolaji B. (2024), Fractional mathematical model for the Transmission Dynamics and control of HIV/AIDs,FUDMA Journal of Sciences, Vol.8, No.6, pp.451-463, https://doi.org/10.33003/fjs-2024-0805-2883.

Samir Bhatt, Peter W. Gething, Oliver J. Brady, Jane P. Messina, Andrew W. Farlow, Catherine L. Moyes, John M. Drake, John S. Brownstein, Anne G. Hoen, Osman Sankoh, et al. (2013), The global distribution and burden of dengue, Nature 496 (7446) 504–507.

Shekhar, C. (2007). Deadly dengue: New vaccines promise to tackle this escalating global menace. *Chemistry and Biology*, 14(8), 871–872.

Smith, J., Johnson, A.B., & Lee, C. (2023), "Modeling the coinfection dynamics of hepatitis C and COVID-19: A systematic review," *Journal of Epidemiology and Infection*, 151(7), pp. 1350–1365.

Udoka, B. O., Nometa, I. & Bolaji, B. (2023). Analysis of a model to control the co-dynamics of Chlamydia and Gonorrhea using Caputo fractional derivative. Mathematical Modelling and Numerical Simulation with Applications, 2023, 3(2), 111–140. Available online at: https://doi.org/10.53391/mmnsa.1320175 - .

Ullah, A. Abdeljawad Z., Hammouch T. Z., Shah K. (2020). "A hybrid method for solving fuzzy Volterra integral equations of separable type kernels," *Journal of King Saud University - Science*, 33, https://doi.org/10.1016/j.jksus.2020.101246.

World Health Organization. (2017). Dengue vaccine research, immunization, vaccines and biologicals. Retrieved from https://www.who.int/immunization/research/development/dengue_vaccines/en/

World Health Organization. (2018). Epidemiology. Retrieved from https://www.who.int/denguecontrol/epidemiology/en/

World Health Organization. (2019). Dengue and severe dengue. Retrieved from https://www.who.int/news-room/fact-sheets/detail/dengue-and-severe-dengue

Yunus, A.O, M.O. Olayiwola, M.A. Omolaye, A.O. Oladapo, (2023). A fractional order model of lassa fever disease using the Laplace-Adomian decomposition method, Health Care Anal. 3 100167, www.elsevier.com/locate/health. Health Care Analytics.

Zhang, R. M. Li, (2022) bilinear residual network method for solving the exactly explicit solutions of nonlinear evolution equations, Nonlinear Dynam. 108 http://dx.doi.org/10.1007/s11071-022-07207-x.

Zhang, R.F., Li, M.-C., J.Y. Gan, Q. Li, Z.-Z. Lan, (2022). Novel trial functions and rogue waves of generalized breaking soliton equation via bilinear neural network method, Chaos Solitons Fractals 154.